A Hydrodynamic Model for Dispersive Waves Generated by Bottom Motion

S. R. Pudjaprasetya and S. S. Tjandra

Abstract A numerical scheme based on the staggered finite volume method is presented at the aim of simulating surface waves generated by a bottom motion. Here, we address the 2D Euler equations in which the vertical domain is resolved only by one layer. Under the assumption of horizontally dominant flow, we enhance the conservative scheme for shallow water equations to include bottom motion and to account take into the hydrodynamic pressure term. The resulting scheme can simulate free surface wave generated by downward motion of a bed-section. The result demonstrates the evolution of a negative wave displacement followed by a dispersive wave train. Our numerical results show good agreement with results from the KdV model and experiment by Hammack [3].

1 Introduction

Motivated by the origin of tsunami, this paper investigates surface wave generation by bottom motion. The study of bottom motion generating surface wave has long been an interesting subject of researches, see for instance [1, 2, 4, 5, 9]. Hammack experiment in [3] is used as one of the benchmark test for tsunami generation codes. In the experiment, part of a bottom wave tank was shifted downwards, as result, surface wave is generated which is then propagate to the right. The generated wave produces a long wave of depression followed by a series of short-waves. In the far

S. R. Pudjaprasetya (✉)
Industrial and Financial Mathematics Research Group, Bandung Institute of Technology, Jalan Ganesha 10, Bandung 40132, Indonesia
e-mail: sr_pudjap@math.itb.ac.id

S. S. Tjandra
Industrial Engineering, Parahyangan Catholic University, Jalan Ciumbuleuit 94, Bandung 40141, Indonesia
e-mail: ssudharmatjandra@yahoo.com

J. Fuhrmann et al. (eds.), *Finite Volumes for Complex Applications VII - Methods and Theoretical Aspects*, Springer Proceedings in Mathematics & Statistics 77,
DOI: 10.1007/978-3-319-05684-5_44,

field downstream region, the effects of nonlinearities and frequency dispersion are of the same order. Thus, numerical models for this simulation should combine those two effects. Fuhrman and Madsen in [2] use Boussinesq model for simulating this experiment. Kervella et. al. in [7] study linear and nonlinear 3D models of tsunami generation.

Here, we enhance the staggered conservative scheme for the nonlinear SWE described previously in Stelling and Duinmeijer [10], to incorporate dispersion effect by solving the Euler equations. Here, we implement one layer approximation for the vertical axis. In this article, numerical scheme for the nonlinear SWE is called hydrostatic model, whereas the scheme for solving Euler equations is called hydrodynamic model.

2 Mathematical Model

Consider the Euler equations for the flow of incompressible and inviscid fluid with constant density

$$u_x + w_z = 0 \tag{1}$$

$$u_t + uu_x + wu_z = -g\eta_x - P_x \tag{2}$$

$$w_t + uw_x + ww_z = -P_z \tag{3}$$

with $(u\ w)^T$ is the fluid particle velocity, $P(x, z, t)$ the hydrodynamic pressure term. Let $\eta(x, t)$ denotes the surface elevation measured from the undisturbed water level. And to calculate the bottom motion, we let the bottom topography to depend also on time t, and we denote it as $-d(x, t)$. For horizontally dominant flow, continuity equation appears as a dynamic equation in terms of η and d, which will be formulated below. Integrating (1) with respect to z from $z = -d(x, t)$ to $z = \eta(x, t)$ yields

$$\int_{-d(x,t)}^{\eta(x,t)} u_x \, dz + w]_{-d(x,t)}^{\eta(x,t)} = 0.$$

Kinematic boundary conditions along the free surface $z = \eta(x, t)$ and along the impermeable bottom $z = -d(x, t)$ are $w = \eta_t + u\eta_x$ and $w = -d_t - ud_x$, respectively. Substituting those two conditions, and neglecting the non-linear term yields

$$(\eta + d)_t + u(\eta + d)_x + \int_{-d(x,t)}^{\eta(x,t)} u_x \, dz = 0.$$

Under shallow water assumption, in which horizontal velocity u is independent of z, the integral term can be approximated by $u_x(\eta + d)$, and the continuity equation reads

$$h_t + (hu)_x = 0, \tag{4}$$

where $h = \eta + d$ denoting the water thickness. Recapitulating, the governing equations for hydrodynamic model that will be used in further discussion are (1–4). Without hydrodynamic pressure and for horizontally dominant flow, the equations can be reduced to

$$h_t + (hu)_x = 0, \tag{5}$$
$$u_t + uu_x + g\eta_x = 0, \tag{6}$$

which is the shallow water equations (SWE). In [8] we discuss the staggered finite volume scheme to solve the nonlinear SWE (5, 6). The conservative properties of this staggered scheme and its accuracy and robustness for simulation of rapidly varied flows are discussed in Stelling and Duinmeijer [10], see also [6]. This scheme is then modified in [11] to solve Euler equations with a small number of vertical grid points. As a result, the scheme is able to simulate nonlinear wave phenomena with dispersion. The key issue of this paper is implementing the conservative scheme for the nonlinear shallow water equation with dispersion for simulation of surface wave generated by bottom motion.

3 Hydrostatic Model

In this section we first discuss numerical scheme for the hydrostatic model (5, 6). Consider a computational domain $[0, L]$ with a staggered grid and partition points $x_{1/2} = 0, x_1, \ldots, x_{i-1/2}, x_i, x_{i+1/2}, \ldots, x_{Nx+1/2} = L$. Continuity equation (5) is approximated at cell $[x_{i-\frac{1}{2}}, x_{i+\frac{1}{2}}]$ and momentum equation (6) is approximated at cell $[x_i, x_{i+1}]$. The approximate equations are

$$\frac{dh_i^n}{dt} + \frac{{}^*h_{i+\frac{1}{2}}^n u_{i+\frac{1}{2}}^n - {}^*h_{i-\frac{1}{2}}^n u_{i-\frac{1}{2}}^n}{\Delta x} = 0, \tag{7}$$
$$\frac{du_{i+1/2}^n}{dt} + g\frac{\eta_{i+1}^{n+1} - \eta_i^{n+1}}{\Delta x} + (uu_x)_{i+1/2}^n = 0. \tag{8}$$

In this approximation h is calculated at every full grid points x_i, whereas u at every half grid points $x_{i+\frac{1}{2}}$, see Fig. 1. Since $\eta = h - d$, hence η is also calculated at every full grid points x_i. In (7), terms h are written with * because it needs approximation, and we implement the upwind approximation

$${}^*h_{i+\frac{1}{2}} = \begin{cases} h_i & \text{if } u_{i+1/2} \geq 0 \\ h_{i+1} & \text{if } u_{i+1/2} < 0. \end{cases} \tag{9}$$

Hence, the term ${}^*h_{i+\frac{1}{2}} u_{i+\frac{1}{2}}$ expresses the first order approximation of mass flux at edge $x_{i+\frac{1}{2}}$ for $i = 0, 1, 2, \ldots, Nx$. When the flow is going to the right $u_{i+1/2} \geq 0$,

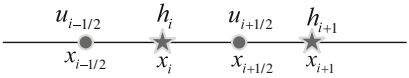

Fig. 1 Staggered grid with configuration of calculated variables h and u

we take the left flux $h_i u_{i+1/2}$, and when the flow is going to the left $u_{i+1/2} < 0$, we take the right flux $h_{i+1} u_{i+1/2}$, and hence mass conservation is always retained in the approximation (7) for any direction of the flow. We note here that bottom motion can be accommodated automatically in this scheme.

For the advection term $(uu_x)_{i+1/2}$ we implement the momentum conservative approximation as introduced by Stelling and Duijnmeijer in [10]. Since $uu_x = \frac{1}{h}\left(\frac{\partial(qu)}{\partial x} - u\frac{\partial q}{\partial x}\right)$ with $q = hu$ the horizontal momentum, a consistent approximation for the advection term is

$$(uu_x)_{i+1/2} = \frac{1}{\bar{h}_{i+\frac{1}{2}}}\left(\frac{\bar{q}_{i+1}\,{}^*u_{i+1} - \bar{q}_i\,{}^*u_i}{\Delta x} - u_{i+\frac{1}{2}}\frac{\bar{q}_{i+1} - \bar{q}_i}{\Delta x}\right), \tag{10}$$

$$\bar{h}_{i+1/2} = \frac{1}{2}(h_i + h_{i+1}), \quad \bar{q}_i = \frac{1}{2}(q_{i+\frac{1}{2}} + q_{i-\frac{1}{2}}), \quad q_{i+\frac{1}{2}} = {}^*h_{i+\frac{1}{2}} u_{i+\frac{1}{2}},$$

with an upwind approximation for ${}^*u_i$

$${}^*u_i = \begin{cases} u_{i-\frac{1}{2}}, & \text{if } \bar{q}_i \geq 0 \\ u_{i+\frac{1}{2}}, & \text{if } \bar{q}_i < 0 \end{cases} \tag{11}$$

Recapitulating, the hydrostatic scheme for the nonlinear SWE are (7, 9) for continuity equation and (8, 10, 11) for the momentum balance. The scheme is of second order accurate for the linear parts, but it is of order one for the non-linear parts, see [8] for details.

4 Hydrodynamic Model

In hydrodynamic formulation, variation in the vertical z-axis is considered, and hence we consider the full set of equations (1–4). The first approximation uses only one layer to resolve the vertical interval, and configuration will be described below. Along the free surface, hydrodynamic pressure is set to zero, and it is increasing with depth. Here, we assume P to be linearly depends on z, and let $P(x_i, z = -d(x_i, t^n), t^n) \equiv P_i^n$. Next, along the impermeable flat bottom holds $w(x, z = -d_0, t) = 0$, and we assume further w to be linearly depends on z. Let $w(x_i, z = \eta(x_i, t^n), t^n) \equiv w_i^n$. Hence, in this hydrodynamic scheme we only need one vector array for dynamic pressure P_i^n and one vector array for vertical velocity w_i^n, which is very efficient. In

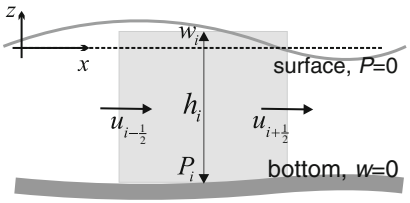

Fig. 2 Configuration of the calculated variables in the staggered grid of hydrodynamic model

the discrete hydrostatic model as explained previously, h are computed at full grid points x_i, whereas u are computed at half grid points $x_{i+1/2}$. In this hydrodynamic model, variables w and P are calculated at full grid points x_i, see Fig. 2.

A way to incorporate the hydrodynamic pressure term is described below. Suppose at any time step, we have calculated η^{n+1}, $\bar{u}$ and $\bar{w}$ from the hydrostatic model, in which $\bar{u}, \bar{w}$ are written in bars since they need corrections. Incorporating the hydrodynamic term, their values are corrected as follows

$$u_{i+\frac{1}{2}}^{n+1} = \bar{u}_{i+\frac{1}{2}} - \Delta t \frac{P_{i+1}^{n+1} - P_i^n}{2\Delta x}, \tag{12}$$

$$w_i^{n+1} = \bar{w}_i + \Delta t \frac{2P_i^{n+1}}{h_i^{n+1}}. \tag{13}$$

But values of P_i should be calculated first. And this can be obtained from one layer approximation of the continuity equation, read as

$$\frac{w_i^{n+1} - 0}{h_i^{n+1}} + \frac{u_{i+\frac{1}{2}}^{n+1} - u_{i-\frac{1}{2}}^{n+1}}{\Delta x} = 0. \tag{14}$$

Substituting (12) and (13) into (14) yields

$$\Delta x \left(w_i^* + \Delta t \frac{2P_i^{n+1}}{h_i^{n+1}} \right) + h_i^{n+1} \left(u_{i+\frac{1}{2}}^* - u_{i-\frac{1}{2}}^* + \Delta t \frac{-P_{i-1}^{n+1} + 2P_i^{n+1} - P_{i-1}^{n+1}}{2\Delta x} \right) = 0 \tag{15}$$

which is a tridiagonal system of equations for P_i^{n+1}.

Finally, the computational procedure when stepping from t_n to t_{n+1} is as follows

1. From the hydrostatic model (7, 8, 10), we calculate η_i^{n+1}, $\bar{u}_{i+\frac{1}{2}}$, and $\bar{w}_i$.
2. Solve the tridiagonal system (15) to calculate P_i^{n+1}.
3. Make correction for $u_{i+\frac{1}{2}}^{n+1}$ using (12).
4. Make correction for w_i^{n+1} using (13).

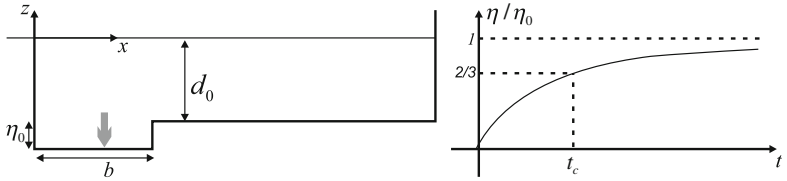

Fig. 3 Bed deformation model: (*left*) spatial deformation (*right*) time deformation

4.1 Hammack Experiment (1973)

The experiment was conducted in a closed wave tank with length 31.6 m, width 39.4 cm. Water depth is $d_0 = 5$ cm. A section of the bed, length b, at the left edge of the water tank was shifted η_0 downwards. This bed motion generates surface elevation in the form of wave depression. This wave is then propagate to the right. Here, we mimic the above experimental set up in our numerical simulation.

The motion of bottom is modelled by

$$d(x,t) = d_0 - \eta_0(1 - e^{-\alpha t})\mathscr{H}(b - x), \tag{16}$$

where $\mathscr{H}$ is the Heaviside function. In [3] this motion is called exponential bottom motion. It depends on parameters η_0 and b which are the amplitude and length of the moving part of the bed, see Fig. 3. Another parameter is the characteristic time t_c which is defined such that $\eta/\eta_0 = \frac{2}{3}$ and parameter α relates with the characteristic time t_c as $\alpha = 1.11/t_c$.

For simulation we take still water level as the initial condition, and a downward bed disturbance according to (16) with $b = 61$ cm, $\eta_0 = -0.5$ cm and $t_c = 0.093b/\sqrt{gd_0}$. Since our scheme can calculate bottom motion, here we perform computations considered as active generation. We take $\Delta x = b/12$ and $\Delta t = 0.001$ s. The choice of Δx is such that $x = b$ is located at a half grid point where we have u value. By doing this, we keep the mass conserved. At the right and left boundaries fully reflecting walls are prescribed, however the simulations are stopped before any reflections occur. As result from a downward bottom motion, water surface moves to a maximum displacement $-\eta_0$. After reaching its maximum, the surface returns to the still water level but it produces an oscillating tail (Fig. 4).

Figure 5 illustrates the downstream behavior of waves resulting from a downward bed displacement. Time series of the waves are recorded at four locations $(x-b)/d_0 = 0, 20, 180, 400$ and the results are plotted w.r.t $t\sqrt{g/d_0} - (x-b)/d_0$. The results of our hydrodynamic scheme are plotted together with Hammack results from two approaches, i.e. KdV model and experimental data. In Fig. 5 (top left) there is no result from the KdV model because it uses passive generation. We observe that the results of our hydrodynamic scheme show a good agreement with results from KdV model as calculated by Hammack [3]. When compared with Hammack

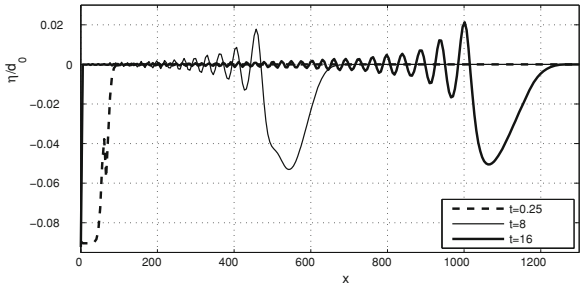

Fig. 4 Snapshots of surface elevation at subsequent time $t = 0.25$, $t = 8$, $t = 16$

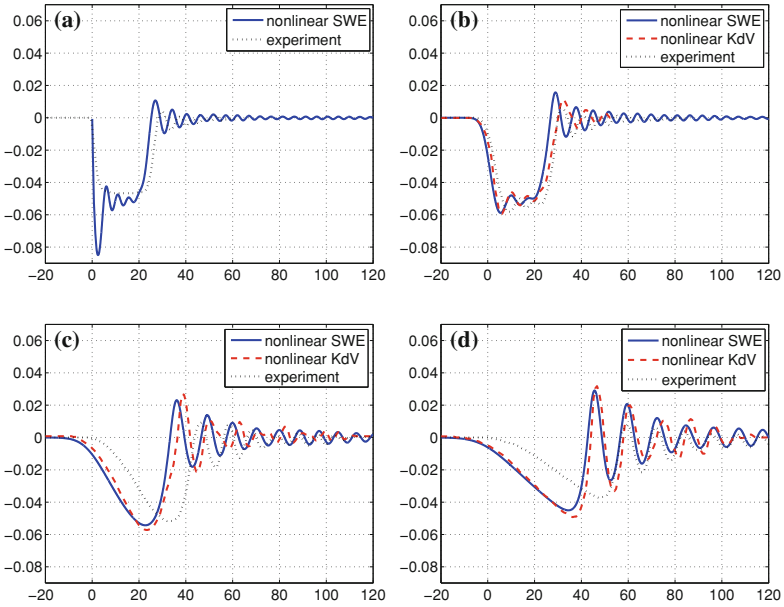

Fig. 5 Time series of surface elevation η/d_0 w.r.t $t\sqrt{g/d_0} - (x-b)/d_0$ resulting from a downward bottom motion. The waves are recorded at locations **a** $(x-b)/d_0 = 0$, **b** 20, **c** 180, **d** 400

experiment [3], the experimental waves have the same shape as predicted by the numerical models. However, in the far field the experimental waves noticeably faster than the numerical models. Further study and comparisons using various bottom motions are still under research, and will be reported in a separate paper.

5 Conclusions

We have presented the non-hydrostatic numerical scheme to calculate surface wave dynamics by solving the 2D Euler equations for horizontally dominant flow. The scheme was used for simulating surface wave generation due to a downward bottom motion. By resolving the vertical axis as just one layer, our hydrodynamic scheme can produce a negative wave displacement followed with a dispersive wave train. Our results are in a good agreement with results from KdV model, also comparable with experimental data. Both are taken from Hammack [3]. Considering these good agreements, we expect our hydrodynamic model is suitable for simulating wave generation by bottom motion. Moreover, it is expected that the proposed method can be computationally competitive with dispersive models like KdV or Boussinesq.

Acknowledgments Financial support from Riset Desentralisasi ITB 2014 and DIKTI scholarship are greatly acknowledged.

References

1. Dutykh, D., Dias, F.: Energy of tsunami waves generated by bottom motion. Proc. R. Soc. A **465**, 725–744 (2009)
2. Fuhrman, D.R., Madsen, P.A.: Tsunami generation, propagation, and run up with high order Boussinesq model. Coast. Eng. **56**, 747–758 (2009)
3. Hammack, J.L.: A note on tsunamis: their generation and propagation in an ocean of uniform depth. J. Fluid Mech. **4**, 769–799 (1973)
4. Hammack, J.L., Segur, H.: The Korteweg-de Vries equation and water waves, part 2. Comparison with experiment. J. Fluid Mech. **65**, 289–314 (1974)
5. Hammack, J.L., Segur, H.: The Korteweg-de Vries equation and water waves, part 3. Oscillatory waves. J. Fluid Mech. **84**, 337–358 (1978)
6. Jochen, K.: Ocean Modelling for Beginners. Springer, London (2009).
7. Kervella, Y., Dutykh, D., Dias, F.: Comparison between three-dimensional linear and nonlinear tsunami generation models. Theor. Comput. Fluid Dyn. **21**, 245–269 (2007)
8. Pudjaprasetya, S.R., Magdalena, I.: Momentum conservative scheme for shallow water flows. East Asian J. Appl. Math. (EAJAM). **4**(2), 152–165 (2014)
9. Saito, T., Furumura, T.: Three-dimensional tsunami generation simulation due to sea-bottom deformation and its interpretation based on the linear theory. Geophys. J. Int. **178**, 877–888 (2009)
10. Stelling, G.S., Duinmeijer, S.P.A.: A staggered conservative scheme for every Froude number in rapidly varied shallow water flows. Int. J. Numer. Methods Fluids **43**, 1329–1354 (2003)
11. Stelling, G.S., Zijlema, M.: An accurate and efficient finite difference algorithm for non hydrostatic free surface flow with application to wave propagation. Int. J. Numer. Methods Fluids **43**, 1–23 (2003)